

UCSF

UC San Francisco Previously Published Works

Title

HIF signaling in osteoblast-lineage cells promotes systemic breast cancer growth and metastasis in mice

Permalink

<https://escholarship.org/uc/item/5d53s06g>

Journal

Proceedings of the National Academy of Sciences of the United States of America, 115(5)

ISSN

0027-8424

Authors

Devignes, Claire-Sophie
Aslan, Yetki
Brenot, Audrey
et al.

Publication Date

2018-01-30

DOI

10.1073/pnas.1718009115

Peer reviewed



HIF signaling in osteoblast-lineage cells promotes systemic breast cancer growth and metastasis in mice

Claire-Sophie Devignes^a, Yetki Aslan^a, Audrey Brenot^{b,1}, Audrey Devillers^a, Koen Schepers^c, Stéphanie Fabre^a, Jonathan Chou^b, Amy-Jo Casbon^b, Zena Werb^{b,2,3}, and Sylvain Provot^{a,2,3}

^aINSERM U1132, Hôpital Lariboisière, 75010 Paris, France; ^bDepartment of Anatomy, University of California, San Francisco, CA 94143; and ^cDepartment of Immunohematology and Blood Transfusion, Leiden University Medical Center, 2300RC Leiden, The Netherlands

Contributed by Zena Werb, December 13, 2017 (sent for review October 13, 2017; reviewed by Florent Eleftheriou and Ernestina Schipani)

Bone metastasis involves dynamic interplay between tumor cells and the local stromal environment. In bones, local hypoxia and activation of the hypoxia-inducible factor (HIF)-1 α in osteoblasts are essential to maintain skeletal homeostasis. However, the role of osteoblast-specific HIF signaling in cancer metastasis is unknown. Here, we show that osteoprogenitor cells (OPCs) are located in hypoxic niches in the bone marrow and that activation of HIF signaling in these cells increases bone mass and favors breast cancer metastasis to bone locally. Remarkably, HIF signaling in osteoblast-lineage cells also promotes breast cancer growth and dissemination remotely, in the lungs and in other tissues distant from bones. Mechanistically, we found that activation of HIF signaling in OPCs increases blood levels of the chemokine C-X-C motif ligand 12 (CXCL12), which leads to a systemic increase of breast cancer cell proliferation and dissemination through direct activation of the CXCR4 receptor. Hence, our data reveal a previously unrecognized role of the hypoxic osteogenic niche in promoting tumorigenesis beyond the local bone microenvironment. They also support the concept that the skeleton is an important regulator of the systemic tumor environment.

breast cancer | bone | metastasis | hypoxia | HIF

Bone is an active tissue in which osteoblasts synthesize and osteoclasts degrade a collagen-rich extracellular matrix, ensuring continuous bone remodeling throughout life. Bone metastasis is a complex process involving crosstalk between disseminated tumor cells and the bone microenvironment, where osteoblasts play a crucial role in promoting breast cancer cell seeding and growth (1–4). Osteoblasts act either indirectly by stimulating bone resorption through osteoclasts (2, 3), which releases growth factors embedded in the bone matrix, or more directly by secreting chemoattractant factors (1) or establishing cell–cell contacts through adherent junctions with breast cancer cells (4). However, our understanding of the complex cellular and molecular mechanisms underlying the tumorigenic effect mediated by the osteoblasts remains incomplete.

Osteoblast-lineage cells comprise cells of different degrees of differentiation that are associated with distinct gene-expression profiles, cell morphologies, and locations in bones (5). These cells derive from osteoprogenitor cells (OPCs), which highly express osterix (OSX) (6, 7) and C-X-C motif chemokine ligand 12 (CXCL12, also called “stromal cell-derived factor 1”) (8). OPCs are found in restricted areas of high bone anabolic activity, predominantly close to the growth plate cartilage and along the metaphyseal cortical bone (6, 7). OPCs differentiate into post-mitotic osteoblasts that express type I collagen and that are evenly distributed within the bone tissue. Osteoblasts finally become terminally differentiated osteocytes. It is unclear whether all osteoblast-lineage cells or only a subset of them could promote bone metastasis locally. Importantly, it is also unknown whether osteoblasts could directly stimulate tumor progression beyond the bone microenvironment. Notably, studies in mice have shown that osteoblasts regulate multiple systemic physiologic processes, such as insulin secretion in the pancreas (9), testosterone synthesis in the testes (10), and brain development (11), in addition to producing bone. This raises the possibility that the osteoblast lineage

could be also involved in the pathogenesis of various organs or tissues. Interestingly, osteoblast-lineage cells express high levels of CXCL12 and receptor activator of nuclear factor κ -B ligand (RANKL) (8, 12), two cytokines circulating in blood and known to stimulate mammary tumor growth and dissemination by binding to their respective receptors, C-X-C chemokine receptor type 4 (CXCR4) and RANK, which are often overexpressed in breast cancers (13, 14). It is therefore conceivable that osteoblast-lineage cells could promote tumor progression beyond bone. Hence, we wondered if altering the signaling pathways essential in bone biology would affect breast cancer growth and dissemination to the bone and beyond.

In bones, tissue hypoxia stabilizes and activates the hypoxia-inducible factor (HIF)1 α , which is essential to maintain bone homeostasis (15–17). Gene inactivation of *Hif1 α* in osteoblasts decreases bone mass and osteoblast numbers. Conversely, osteoblast-specific ablation of the ubiquitin ligase VHL encoded by the tumor-suppressor gene *von Hippel Lindau (Vhlh)*, which targets HIF1 α and HIF2 α to the proteasome for degradation (18), leads to overactivation of HIF signaling in the osteoblast lineage and increases bone mass (15–17). HIF2 α is also expressed in osteoblasts and is stabilized upon ablation of VHL (15). However, in contrast to HIF1 α , mice lacking HIF2 α in osteoblasts present only a modest decrease in trabecular bone volume (16).

Hypoxia and HIF signaling constitute important components of the tumor microenvironment (19), promoting primary breast

Significance

Previous work showed that primary tumors instigate systemic macroenvironmental changes supporting cancer progression and metastasis. Here, we show that activation of HIF signaling in osteoblast-lineage cells also generates systemic changes promoting breast cancer growth and dissemination in bones and outside the skeleton. Our results indicate that loss of bone homeostasis through alterations of the bone anabolism could affect breast cancer progression and present the skeleton as an important organ of the tumor macroenvironment. They also suggest that targeting the bone microenvironment could limit systemic tumor growth and dissemination in breast cancer.

Author contributions: Z.W. and S.P. designed research; C.-S.D., Y.A., A.B., A.D., K.S., S.F., and S.P. performed research; K.S., J.C., A.-J.C., and S.P. contributed new reagents/analytic tools; C.-S.D., Z.W., and S.P. analyzed data; and C.-S.D., J.C., Z.W., and S.P. wrote the paper.

Reviewers: F.E., Baylor College of Medicine; and E.S., University of Michigan.

The authors declare no conflict of interest.

Published under the PNAS license.

¹Present address: Department of Medicine, Institute for Community and Civic Engagement, Washington University School of Medicine, St. Louis, MO 63110.

²Z.W. and S.P. contributed equally to this work.

³To whom correspondence may be addressed. Email: zena.werb@ucsf.edu or sylvain.provot@inserm.fr.

This article contains supporting information online at www.pnas.org/lookup/suppl/doi:10.1073/pnas.1718009115/-DCSupplemental.

tumor dissemination to several tissues, including to bones (20, 21). However, whether local hypoxia in bones and the activation of HIF signaling in osteoblast-lineage cells influence breast cancer cells is unknown. Because hypoxia supports osteoblastogenesis (15–17), and osteoblasts promote bone metastasis (1–4), we hypothesized that activation of HIF signaling in osteoblasts would promote breast cancer cell metastasis to bones and would promote distant mammary tumor growth and dissemination beyond bones.

Results

Breast Cancer Cells Disseminate near Hypoxic Osteoprogenitors. To better characterize the cellular and molecular mechanisms that could favor metastasis of breast cancer cells to bone, we first evaluated where the earliest colonization process takes place in the bone marrow. We reasoned that if only a subset of osteoblast-lineage cells promoted bone metastasis, tumor cells would disseminate preferentially near this cell population in bones. Previous reports showed that bone metastases are observed in areas of high bone turnover (3), enriched in osteoblasts (2, 4), and located near the cortical bone or within the trabecular bone next to the growth plate cartilage. Interestingly, this is also where the majority of OPCs are observed (Fig. 1A) (6, 7), sug-

gesting a potential interaction of these cells with breast cancer cells in the early dissemination process. We tested this possibility by intracardiac (i.c.) injections of a breast cancer cell line [generated from a breast carcinoma induced by expression of the polyoma virus middle T (PyMT) oncoprotein (22)] expressing GFP and luciferase (BCC-GFP::LUC) into syngeneic immunocompetent recipient mice (Fig. S1). We analyzed early tumor dissemination only 5 d after injection to assess the initial location of disseminated cells. We found early metastases in areas within trabecular bones below the growth plate cartilage that were significantly enriched in OPCs (Fig. 1A and B). Disseminated cells were never found in areas further down the metaphyseal bone (toward the epiphysis) that have fewer or no OPC (Fig. 1B). Thus, breast cancer cells preferentially disseminate near OPCs. Importantly, we found that OSX⁺ OPCs are highly hypoxic (Fig. 1C and D) and express HIF1 α and, to a lesser extent, HIF2 α (Fig. 1E and F). Together, these data raise the possibility that activation of HIF signaling in OPCs favors early dissemination of breast cancer cells to bone.

HIF Signaling in Osteoblast Lineage Increases Bone Mass and Bone Metastasis Locally. To test the possibility that HIF signaling in OPCs or in descending osteoblast-lineage cells might contribute

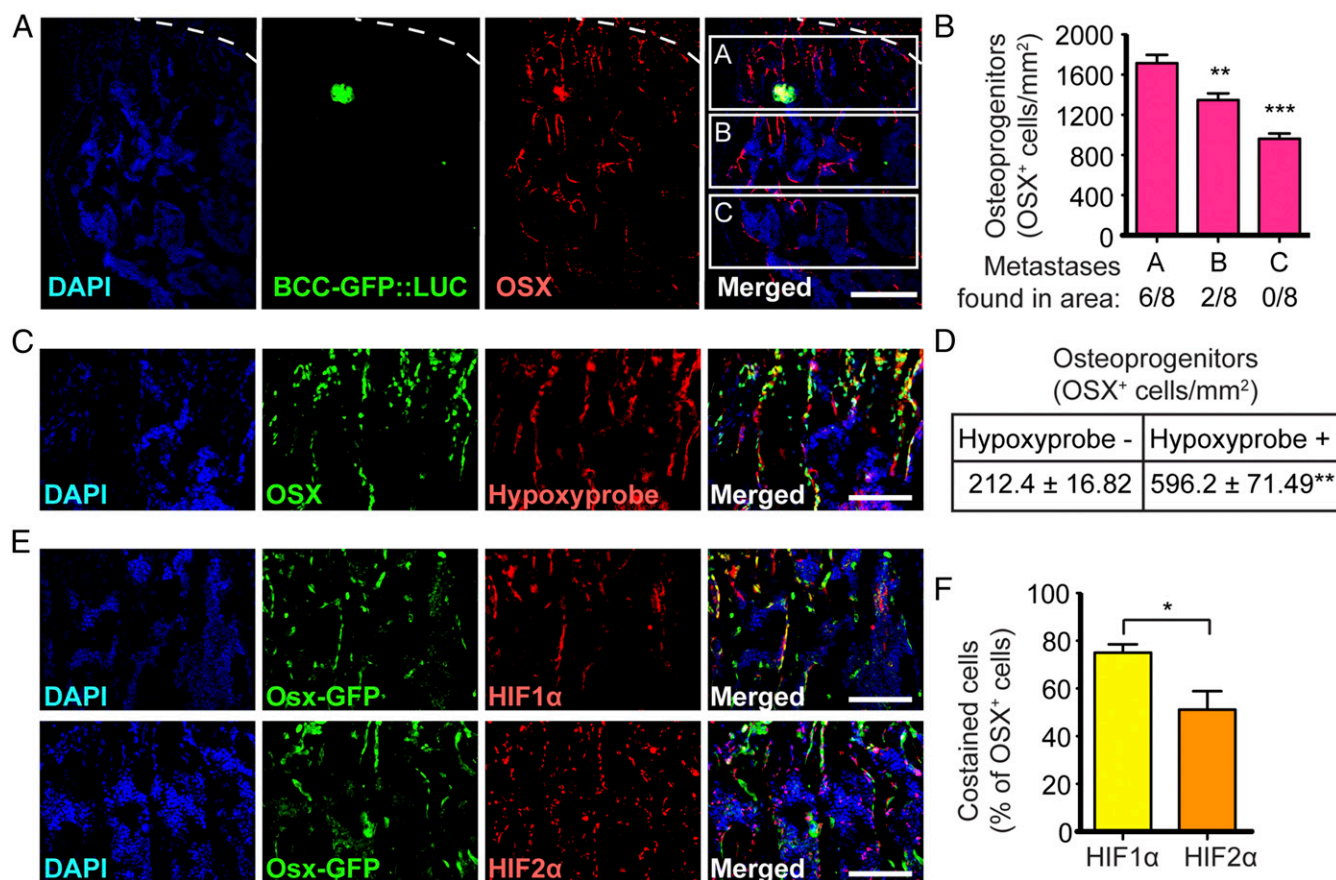


Fig. 1. Breast cancer cells disseminate near hypoxic osteoprogenitor cells. (A) Immunohistochemistry showing GFP-expressing breast cancer cells (BCC-GFP::LUC) in green and OPCs, detected by anti-OSX immunostaining in red, in a wild-type mouse hind limb 5 d after i.c. injection. Dashed lines indicate the limit between the cartilage growth plate (above the dashed line) and the bone (below the dashed line). (B) Quantification of OSX⁺ cells and distribution of bone metastases in three areas (A, B, and C) below the growth plate cartilage; $n = 8$ independent bone metastases obtained from three mice 5 d after i.c. injections. (C) Immunohistochemistry showing that OSX expression (in green) colocalizes with hypoxia (Hypoxyprobe, in red) in hind limb sections of a wild-type mouse. (D) Quantification of OSX⁺ cells costained with Hypoxyprobe, showing that a majority of OPCs are hypoxic; $n = 3$ mice. (E) Immunohistochemistry showing that GFP expression driven by the *Osx* promoter (*Osx*-GFP, which marks OPCs, in green) colocalizes with HIF1 α (in red; *E*, Upper Row) and HIF2 α (in red; *E*, Lower Row) in the hind limbs of *Osx*-Cre::GFP transgenic mice. (F) Quantification of OSX⁺ cells expressing HIF1 α or HIF2 α ; $n = 3$ mice with two sections per mouse. (Scale bars: 200 μ m in A; 100 μ m in C and E.) Values indicate the mean \pm SEM, * $P < 0.05$, ** $P < 0.01$, *** $P < 0.0001$, two-tailed Student's *t* test.

to bone metastasis, we conditionally inactivated *Hif1 α* in OPCs by crossing mice expressing Cre fused to GFP under the *Osterix* promoter (*Osx-Cre::GFP*) (23) to *Hif1 α* floxed (*Hif1 α ^{fl/fl}*) (24) mice, generating $\Delta Hif1\alpha^{OSX}$ mice. *Osx-Cre* is a well-characterized transgene that targets OPCs. We verified that *Osx-Cre::GFP* drives the expression of *CRE::GFP* and efficiently recombines floxed alleles in skeletal tissue but not in the mammary gland or in other organs commonly colonized by breast cancer cells (lungs, liver, and others) or in hematopoietic cells (Fig. 1E and Fig. S2).

As previously reported (15), we observed that $\Delta Hif1\alpha^{OSX}$ mice have reduced bone mass (Fig. 2A and B). We tested the role of osteoblast-specific HIF signaling in bone metastasis by inoculating $\Delta Hif1\alpha^{OSX}$ mice with syngeneic BCC-GFP::LUC cells by i.c. injection and assessing their ability to colonize bones. We observed that $\Delta Hif1\alpha^{OSX}$ mice developed bone metastases less frequently than control animals (Fig. 2C). To recapitulate the entire metastatic process, we also transplanted BCC-GFP::LUC cells orthotopically into mammary fat pads (i.f.p.) and evaluated whether tumor cells disseminate from primary mammary tumors to the bones. $\Delta Hif1\alpha^{OSX}$ mice developed spontaneous bone metastases less frequently than control animals (Fig. 2D). Hence, ablating HIF signaling in osteoblast-lineage cells suppresses metastasis to the bones.

To assess the effect of activating HIF signaling in osteoblast-lineage cells on bone metastasis, we conditionally inactivated *Vhlh* in OPCs by crossing *Osx-Cre::GFP* to *Vhlh* floxed (*Vhlh^{fl/fl}*) mice (25), generating $\Delta Vhlh^{OSX}$ mice. As previously reported (15), we observed that $\Delta Vhlh^{OSX}$ mice have dramatically increased bone volume (Fig. 2A and B). $\Delta Vhlh^{OSX}$ mice developed bone metastases more frequently and more rapidly than control animals after i.c. injections (Fig. 2E) and orthotopic transplantations (Fig. 2D). Notably, similar results were obtained after i.c. injections of NT2.5 breast cancer cells derived from Neu/HER2 transgenic mice (Fig. S3A and B) (26). Taken together, these results demonstrate that activation of HIF signaling in osteoblast-lineage cells promotes breast cancer cell colonization of the bones.

HIF Signaling in Osteoblast Lineage Promotes Systemic Breast Cancer Growth and Dissemination. We next examined the systemic influence of the bone microenvironment on tumor growth in the breast and assessed metastatic colonization of distant organs, other than bones. Strikingly, $\Delta Hif1\alpha^{OSX}$ mice developed significantly smaller primary tumors after orthotopic transplantation (Fig. 3A and B). Conversely, $\Delta Vhlh^{OSX}$ mice developed much larger primary tumors (Fig. 3C and D). Similar results were obtained using NT2.5 breast cancer cells (Fig. S3C and D). Mammary tumors collected from mutant mice after orthotopic transplantation were histologically similar to those obtained from control animals but had decreased cell proliferation in $\Delta Hif1\alpha^{OSX}$ mice and increased cell proliferation in $\Delta Vhlh^{OSX}$ mice (Fig. 3E and F). These results demonstrate that the bone affects breast cancer remotely in the mammary gland. Interestingly, relatively soon after orthotopic transplantations, we detected disseminated BCC-GFP::LUC cells that could correspond to metastases in mandibular bones or in salivary glands in the jaw area of $\Delta Vhlh^{OSX}$ mice (Fig. 3C) but never in control mice, even after controlling for primary tumor size. This indicates that $\Delta Vhlh^{OSX}$ mice present increased tumor dissemination that is not solely due to accelerated primary tumor growth.

To assess metastasis in other organs, we analyzed lung colonization after i.v. injections of BCC-GFP::LUC cells. Similar to our observations in bones, $\Delta Hif1\alpha^{OSX}$ mice developed lung metastases less frequently, and $\Delta Vhlh^{OSX}$ mice developed lung metastases more frequently and rapidly than controls after i.v. injections (Fig. 3G–J). Moreover, i.c. injections revealed that, in addition to bones and lungs, numerous other organs commonly targeted by disseminated breast cancer cells were rapidly colonized in $\Delta Vhlh^{OSX}$ mice (Fig. 3M and N). Conversely, $\Delta Hif1\alpha^{OSX}$ mice showed fewer disseminated tumors after i.c. injection (Fig. 3K and L). Given that the frequency, and not just the size, of metastases was affected, these data indicate that altering HIF signaling in bones alters the capacity of breast cancer cells to invade and colonize other organs.

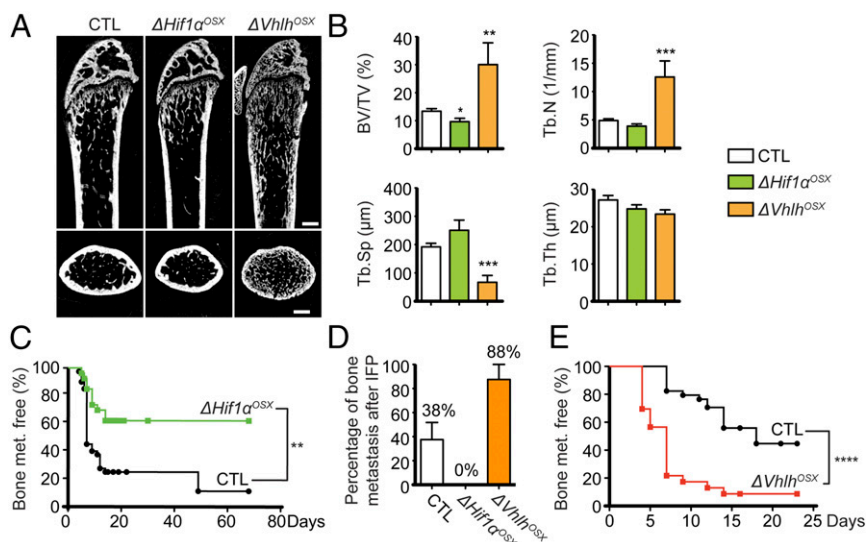


Fig. 2. HIF signaling in osteoblast-lineage cells increases bone mass and bone metastasis. (A) Representative micro-CT images of sagittal (*Upper*) and transversal (*Lower*) views of distal femurs of control (CTL), $\Delta Hif1\alpha^{OSX}$, and $\Delta Vhlh^{OSX}$ mice. (B) Histograms showing histomorphometric analyses of trabecular bone volume over tissue volume (BV/TV), trabecular number (Tb.N), trabecular separation (Tb.Sp), and trabecular thickness (Tb.Th) in control ($n = 9$), $\Delta Hif1\alpha^{OSX}$ ($n = 5$), and $\Delta Vhlh^{OSX}$ ($n = 3$) femurs. (C) Kaplan–Meier analyses of bioluminescence-based detection of bone metastases after i.c. injections of BCC-GFP::LUC in control ($n = 42$) and $\Delta Hif1\alpha^{OSX}$ ($n = 27$) mice. (D) Histogram showing histological detection of bone metastases 30 d after i.f.p. transplantation of BCC-GFP::LUC in control ($n = 12$), $\Delta Hif1\alpha^{OSX}$ ($n = 6$), and $\Delta Vhlh^{OSX}$ ($n = 6$) mice. (E) Kaplan–Meier analyses of bioluminescence-based detection of bone metastases after i.c. injections of BCC-GFP::LUC in control ($n = 34$) and $\Delta Vhlh^{OSX}$ ($n = 23$) mice. (Scale bars: 500 μ m.) Values indicate the mean \pm SEM, * $P < 0.05$, ** $P < 0.01$, *** $P < 0.001$, **** $P < 0.0001$, two-tailed Student's *t* test (B) or log-rank (Mantel–Cox) test (C and E).

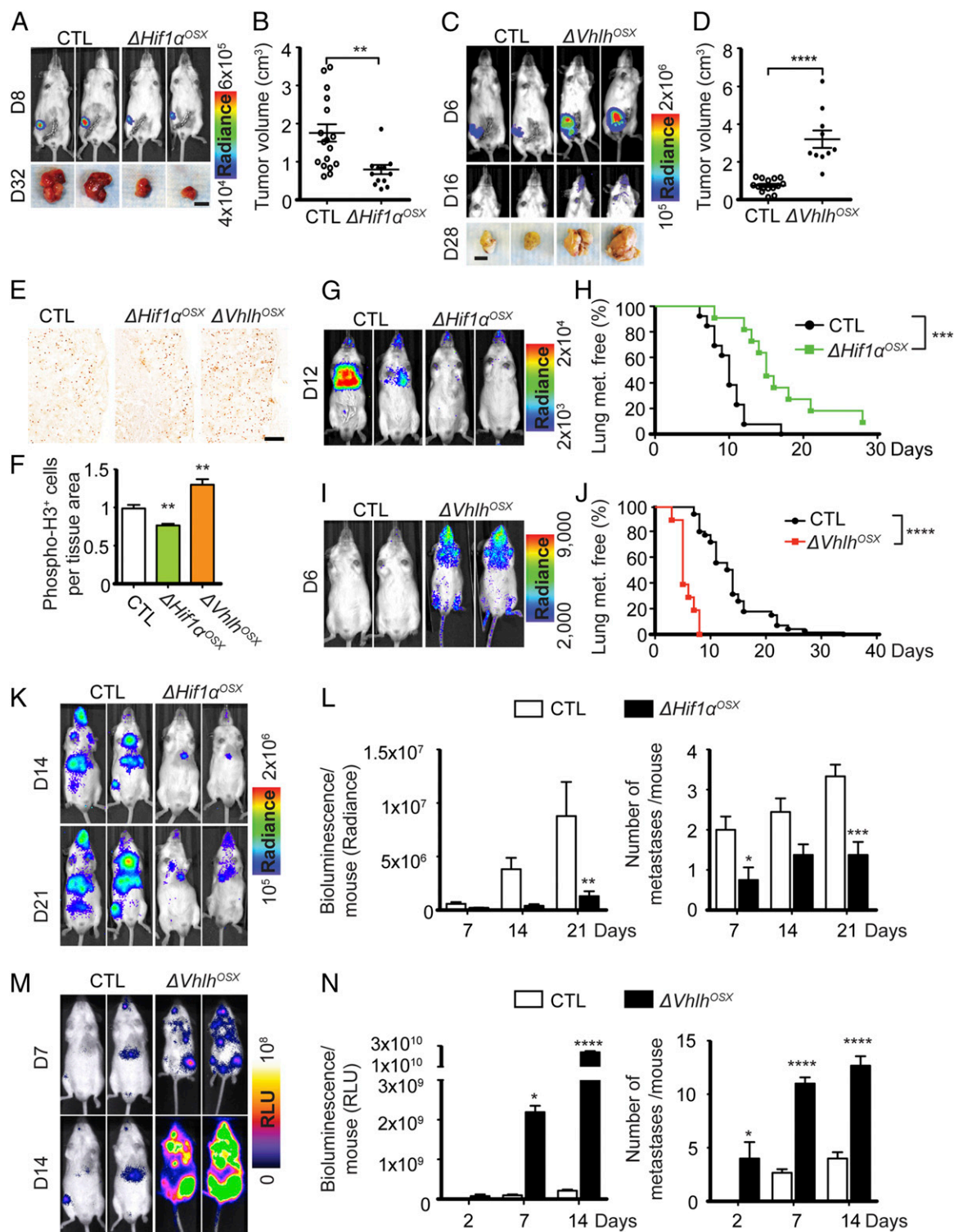


Fig. 3. HIF signaling in osteoblast-lineage cells promotes systemic breast cancer growth and dissemination. (**A** and **B**) Representative bioluminescent images and mammary tumor photographs (**A**) and quantification of tumor volumes (**B**) 32 d after i.f.p. transplantation of 10^5 BCC-GFP::LUC cells in control ($n = 17$) and $\Delta Hif1\alpha^{OSX}$ ($n = 12$) mice. (**C** and **D**) Representative bioluminescent images of mammary tumors and disseminated tumor cells and photographs of mammary tumors (**C**) and quantification of tumor volumes (**D**) 28 d after i.f.p. transplantation of 10^4 BCC-GFP::LUC cells in control ($n = 15$) and $\Delta Vhhl^{OSX}$ ($n = 10$) mice. (**E** and **F**) Representative images of phospho-histone H3 immunostaining showing mitotic cells in mammary tumors harvested 12 d post i.f.p. transplantation (**E**) and quantification of positive cells per tissue area (**F**), normalized to control (control: $n = 7$; $\Delta Hif1\alpha^{OSX}$: $n = 4$; and $\Delta Vhhl^{OSX}$: $n = 6$). (**G** and **I**) Representative bioluminescent images obtained after i.v. injections of BCC-GFP::LUC cells. (**H** and **J**) Kaplan–Meier analyses of lung metastasis after i.v. injections of BCC-GFP::LUC cells in control (**H**: $n = 13$; **J**: $n = 37$) and $\Delta Hif1\alpha^{OSX}$ (**H**: $n = 11$) or $\Delta Vhhl^{OSX}$ mice (**J**: $n = 10$). (**K**–**N**) Representative bioluminescent images (**K** and **M**) and quantification of the total bioluminescent signal per mouse [in relative light units, (RLU) or radiance] and of the number of metastases detected by bioluminescence (**L**: $n = 8$; **N**: $n = 3$) for each group after i.c. injections of BCC-GFP::LUC cells. (Scale bars: 1 cm in **A** and **C**; 200 μ m in **E**.) Values indicate the mean \pm SEM, * $P < 0.05$, ** $P < 0.01$, *** $P < 0.001$, **** $P < 0.0001$, two-tailed Student's *t* test (**B**, **D**, and **F**), log-rank (Mantel–Cox) test (**H** and **J**), or two-way ANOVA (**L** and **N**).

Because *Vhlh* deletion leads to stabilization of both HIF1 α and HIF2 α , we assessed the role of HIF2 α in the systemic pro-tumorigenic effect observed in $\Delta Vhlh^{OSX}$ mice. The genetic inactivation of *Hif2a* in osteoblast-lineage cells did not significantly alter the bone phenotype evaluated by micro-computed tomography (micro-CT) in 8-wk-old mice (Fig. S4A), which is consistent with a previous report (16). $\Delta Hif2a^{OSX}$ mice presented no significant difference in bone metastasis after i.c. injections or in primary mammary tumor growth after orthotopic transplantation (Fig. S4 B–E). In addition, inactivation of *Hif1a* in $\Delta Vhlh^{OSX}$ mice, which partially reduced increased bone mass (Fig. S4F), reverted the effect on increased tumorigenesis (Fig. S4 G–J). Collectively, our results demonstrate that activation of HIF signaling in osteoblast-lineage cells exerts a systemic control of mammary tumor growth and metastasis beyond the bone microenvironment and suggest that this effect depends primarily on HIF1 α rather than on HIF2 α . These results are consistent with the fact that OSX⁺ OPCs preferentially express HIF1 α , not HIF2 α (Fig. 1 E and F).

Osteoclasts Do Not Mediate Systemic Breast Cancer Growth and Dissemination in $\Delta Vhlh^{OSX}$ Mice. To explain our finding, we hypothesized that OPC-induced alterations in the bone microenvironment lead to the release of molecules stimulating tumor growth and dissemination in the bloodstream. We assumed that these molecular cues were quantitatively altered in mutant mice. We therefore thoroughly analyzed the bone phenotype of these mice to identify local changes that could explain the systemic effect on tumor growth.

The decreased bone mass observed in $\Delta Hif1a^{OSX}$ mice was associated with a significant decrease in osteoblast numbers (Fig. 4A). Conversely, $\Delta Vhlh^{OSX}$ mice with high bone mass had increased osteoblast numbers (Fig. 4B). Osteoblasts stimulate osteoclast differentiation by secreting RANKL to ensure bone homeostasis (27). Accordingly, we observed that increased osteoblast numbers led to increased osteoclast numbers in $\Delta Vhlh^{OSX}$ mice (Fig. 4D) and increased serum levels of deoxy-pyridinoline, a marker of bone resorption (Fig. 4C). However, the ratios of osteoclasts to bone surface area in $\Delta Vhlh^{OSX}$ and $\Delta Hif1a^{OSX}$ mice were comparable to those in controls (Fig. 4D). Moreover, we observed unresorbed cartilage remnants in the primary spongiosa of $\Delta Vhlh^{OSX}$ bones, which could result from steric hindrance by osteoid deposition (Fig. 4E) or altered osteoclast function in these mice (Fig. 4F). Together, these data suggested that osteoclast activity might not mediate the systemic tumorigenic effect of the skeleton in mutant mice. Nonetheless, we tested the possibility that activation of HIF in OPCs could indirectly stimulate tumor growth in bones and beyond through osteoclasts in $\Delta Vhlh^{OSX}$ mice. To this end, $\Delta Vhlh^{OSX}$ mice were treated with alendronate (ALN), a bisphosphonate commonly used to suppress osteoclast function and bone metastasis (28). The treatment started 2 d before BCC-GFP::LUC inoculation and was maintained until mice were killed. ALN treatment increased bone mass (Fig. S5E) and significantly reduced bone metastasis in control mice after i.c. injections (Fig. S5 A and B). These results are consistent with the ALN-mediated inhibition of bone resorption and bone metastasis previously reported (28). However, ALN treatment did not affect bone metastasis after i.c. injections or primary tumor growth after orthotopic transplantation in $\Delta Vhlh^{OSX}$ mice (Fig. S5 A–D). These results argue against the possibility that osteoclasts play a major role in mediating the systemic tumorigenic effects observed in these mice.

Bone-Derived VEGF Does Not Mediate Systemic Breast Cancer Growth and Dissemination in $\Delta Vhlh^{OSX}$ Mice. Previous work showed that HIF signaling induces VEGF expression in osteoblast-lineage cells (15). Accordingly, activation of HIF signaling in OPCs was associated with significantly increased angiogenesis in $\Delta Vhlh^{OSX}$

bones, while angiogenesis was decreased in $\Delta Hif1a^{OSX}$ bones (Fig. S6A). Although VEGF and increased angiogenesis could support bone metastasis locally in $\Delta Vhlh^{OSX}$ mice, it was not clear whether VEGF would be released systemically to increase angiogenesis and promote tumor growth and dissemination away from bones. We found no significant changes in VEGF levels in the plasma of $\Delta Vhlh^{OSX}$ and $\Delta Hif1a^{OSX}$ mice (Fig. S6B). Moreover, we observed a slight but significant decrease in vascular invasion in mammary tumors obtained from $\Delta Vhlh^{OSX}$ mice and no change in those obtained from $\Delta Hif1a^{OSX}$ mice (Fig. S6 C and D). Together, our data strongly suggest that systemic tumor growth and dissemination induced by the skeleton in mutant mice are not mediated by VEGF-induced angiogenesis outside the skeleton.

CXCL12 Mediates Systemic Breast Cancer Growth and Dissemination Induced by the Skeleton. We noticed that 8-wk-old $\Delta Vhlh^{OSX}$ mice have large amounts of unmineralized bone matrix called “osteoid” (Fig. 4E), which likely reflects the expansion of undifferentiated bone marrow stromal cells observed in these mice (Fig. 4F) rather than a defect in bone mineralization. Consistent with this observation, we observed a dramatic accumulation of OSX⁺ OPCs in these mice (Fig. 4 G and H). Conversely, the number of OSX⁺ OPCs was decreased in $\Delta Hif1a^{OSX}$ mice (Fig. 4 G and H). To test whether skeletal progenitors could directly influence breast cancer cell growth and dissemination, we performed cocultures of primary mesenchymal stem/progenitor cells (MSPCs) and breast cancer cells in which each cell type was physically separated by a microporous membrane. MSPCs were able to significantly stimulate breast cancer cell migration and proliferation (Fig. 4I). This effect was reduced with MSPCs derived from $\Delta Hif1a^{OSX}$ mice and was increased with MSPCs derived from $\Delta Vhlh^{OSX}$ mice (Fig. 4I).

CXCL12 is highly expressed in OSX⁺ OPCs, rather than in mature osteoblasts (8), and its expression is induced by hypoxia through HIF1 α in several cell types (29–32). Interestingly, *Cxcl12* mRNA expression in bone was significantly higher than that of the cells in bone marrow or in mammary tumors (Fig. 5A), indicating that bones might constitute an important source of CXCL12. MSPCs expressed higher CXCL12 levels than cultured bone marrow cells, MC3T3 osteoblasts, MLO-Y4 osteocytes, or primary chondrocytes (Fig. 5B). We also observed that hypoxia exposure of bone explants depleted of hematopoietic cells up-regulated CXCL12 expression to the same extent as phosphoglycerate kinase 1 (PGK1), a bona fide target gene of HIF1 α (Fig. 5C). This effect was significantly reduced in bone explants derived from $\Delta Hif1a^{OSX}$ mice, demonstrating that HIF1 α up-regulates CXCL12 expression in osteoblast-lineage cells exposed to hypoxia. Importantly, we observed a significant increase in the number of CXCL12⁺ OPCs in the bones of $\Delta Vhlh^{OSX}$ mice (Fig. 5 D and E), consistent with the dramatic increase in OSX⁺ cells in these mice. Conversely, decreased OSX⁺ cell numbers in the bones of $\Delta Hif1a^{OSX}$ mice were associated with fewer CXCL12⁺ OPCs (Fig. 5 D and E). Notably, we found that $\Delta Vhlh^{OSX}$ mice displayed a nearly 50% increase in plasma levels of CXCL12 (Fig. 5F). The increased circulating CXCL12 levels in $\Delta Vhlh^{OSX}$ mice did not come from lungs, mammary glands, or mammary tumors (Fig. 5G) and was remarkable, given the few cells initially targeted by our conditional knockout. Despite the decreased number of CXCL12⁺ OPCs in the bones of $\Delta Hif1a^{OSX}$ mice (Fig. 5 D and E), we could not detect a decrease in CXCL12 concentrations in the plasma of these mice (Fig. 5F), presumably due to low basal levels in the control mice and the limit of sensitivity of the assay that failed to measure lower concentrations of CXCL12.

These alterations of CXCL12⁺ OPC numbers and circulating levels of CXCL12 were interesting, since CXCL12 can promote mammary tumor cell growth and dissemination (13) (Fig. S7C).

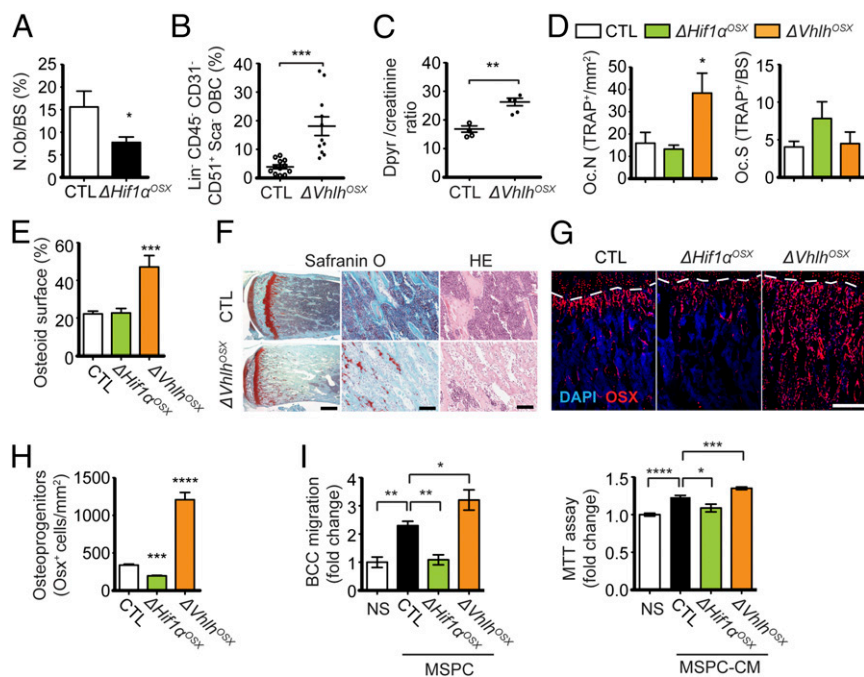


Fig. 4. HIF signaling controls the pool of skeletal progenitors, which directly promotes breast cancer cell migration and proliferation. (A) Quantification of osteoblast numbers expressed as the percentage of bone surface in control ($n = 6$) and $\Delta Hif1\alpha^{OSX}$ ($n = 7$) mice. (B) FACS analysis of lineage-negative (Lin^{-}) $CD45^{-} CD31^{-} CD51^{+} Sca1^{-}$ osteoblast-lineage cells (OBCs) from crushed bones of control ($n = 12$) and $\Delta Vhhl^{OSX}$ ($n = 11$) mice, expressed as percentages of total cells. (C) Dosage of deoxyypyridinoline normalized to creatinine in urine of control ($n = 4$) and $\Delta Vhhl^{OSX}$ ($n = 5$) mice. (D) Histomorphometric analysis of tartrate-resistant acid phosphatase-positive (TRAP⁺) osteoclast numbers per tissue area (Oc.N) or per bone surface area (Oc.S) in control ($n = 8$), $\Delta Hif1\alpha^{OSX}$ ($n = 5$), and $\Delta Vhhl^{OSX}$ ($n = 3$) mice. (E) Histomorphometric quantifications of the osteoid surface (immature bone) done on 8-wk-old femur sections stained with toluidine blue. Values are expressed as the percentage of bone surface in control ($n = 9$), $\Delta Hif1\alpha^{OSX}$ ($n = 6$), and $\Delta Vhhl^{OSX}$ ($n = 3$) mice. (F) Representative images of Safranin O staining of mouse hind limbs showing increased unmineralized bone matrix (stained in light blue) and cartilage remnants (stained in red) in the metaphyseal area of $\Delta Vhhl^{OSX}$ bone. H&E (HE) staining reveals fibrotic tissues with expansion of undifferentiated stromal cells in the metaphyseal area of $\Delta Vhhl^{OSX}$ hind limbs. (G) Immunostaining showing OSX⁺ OPCs (in red) in mouse hind limbs. Dashed lines indicate the limit between cartilage (above the dashed line) and bone (below the dashed line). (H) Quantification of OSX⁺ cells per tissue area ($n = 3$). (I) Migration assay (Left) and 3-[4,5-dimethylthiazol-2-yl]-2,5-diphenyltetrazolium bromide (MTT) assay (Right) with BCC-GFP::LUC cells (BCC) not stimulated (NS: serum-free medium) or cocultured with MSPCs (Left) or stimulated with MSCP-conditioned medium (MSPC-CM, Right) derived from control ($n = 4$), $\Delta Hif1\alpha^{OSX}$ ($n = 3$), and $\Delta Vhhl^{OSX}$ ($n = 4$) mice. Values are normalized to NS controls. (Scale bars: 1 mm in F, Left; 100 μ m in F, Middle and Right; 200 μ m in G.) Values indicate the mean \pm SEM, * $P < 0.05$, ** $P < 0.01$, *** $P < 0.001$, **** $P < 0.0001$, two-tailed Student's *t* test.

Therefore, CXCL12 produced by hypoxic OPCs might serve as the link between the skeleton and systemic tumor growth and metastasis. Consistent with this idea, knocking down CXCL12 with siRNAs (siCxcl12) in MSPCs significantly reduced breast cancer cell migration and proliferation (Fig. 5 H and I). Hence, CXCL12 derived from skeletal progenitors can directly stimulate breast cancer cell migration and proliferation in vitro, further suggesting that CXCL12 could directly stimulate tumor cell growth and dissemination in $\Delta Vhhl^{OSX}$ mice.

CXCR4 and CXCR7, the receptors of CXCL12, are highly expressed in several types of cancer, including breast cancers (13, 33). We observed that our breast cancer cells highly expressed CXCR4 compared with CXCR7 (Fig. S7A), raising the possibility that increased circulating levels of CXCL12 in $\Delta Vhhl^{OSX}$ mice might directly stimulate tumor cell proliferation and dissemination through CXCR4. To test this, we treated control and VHL-mutant mice with the well-characterized inhibitor of CXCR4, AMD3100 (plerixafor) (34), and assessed tumor growth and dissemination. Because AMD3100 has been reported to activate CXCR7 (35), in addition to inhibiting CXCR4, we verified that AMD3100 inhibits the signal-transduction pathways activated downstream of CXCR4 in tumor cells. AMD3100 treatment of BCC-GFP::LUC cells in vitro abolished CXCL12-induced activation of the MAPK-pathway ERK downstream of CXCR4 (Fig. S7B). AMD3100 also abolished breast cancer cell migration and proliferation induced by exogenous CXCL12

(Fig. S7C). Hence, AMD3100 inhibits CXCL12-induced activation of CXCR4 in breast cancer cells. Interestingly, AMD3100 treatment also blunted breast cancer cell migration and proliferation induced by MSPCs in vitro (Fig. 6A). Strikingly, AMD3100 treatment abolished the increased frequency of bone metastases in $\Delta Vhhl^{OSX}$ mice in vivo (Fig. 6B). Moreover, $\Delta Vhhl^{OSX}$ mice treated with AMD3100 developed mammary tumors comparable in size to those of control mice after orthotopic transplantations (Fig. 6C and D). The i.c. injections also revealed that $\Delta Vhhl^{OSX}$ mice treated with AMD3100 showed limited tumor growth globally and, in some cases, tumor regression in numerous organs/tissues usually colonized by breast cancer cells (Fig. 6E and F). Together, these data demonstrate that CXCL12–CXCR4 signaling mediates the systemic increase of breast cancer growth and dissemination observed in $\Delta Vhhl^{OSX}$ mice and suggest that CXCL12 produced by OPCs acts directly through binding to CXCR4 in breast cancer cells.

We tested whether CXCL12 directly stimulates tumor growth and dissemination in vivo by knocking down (KD) CXCR4 in BCC-GFP::LUC cells using shRNAs. This strategy reduced CXCR4 expression in BCC-CXCR4^{KD} cells by ~80% compared with controls (BCC-CTL) (Fig. 6G). We observed that cell proliferation and survival were unaffected in BCC-CXCR4^{KD} cells (Fig. S7D). $\Delta Vhhl^{OSX}$ mice inoculated with BCC-CXCR4^{KD} cells had decreased tumor burden compared with controls after

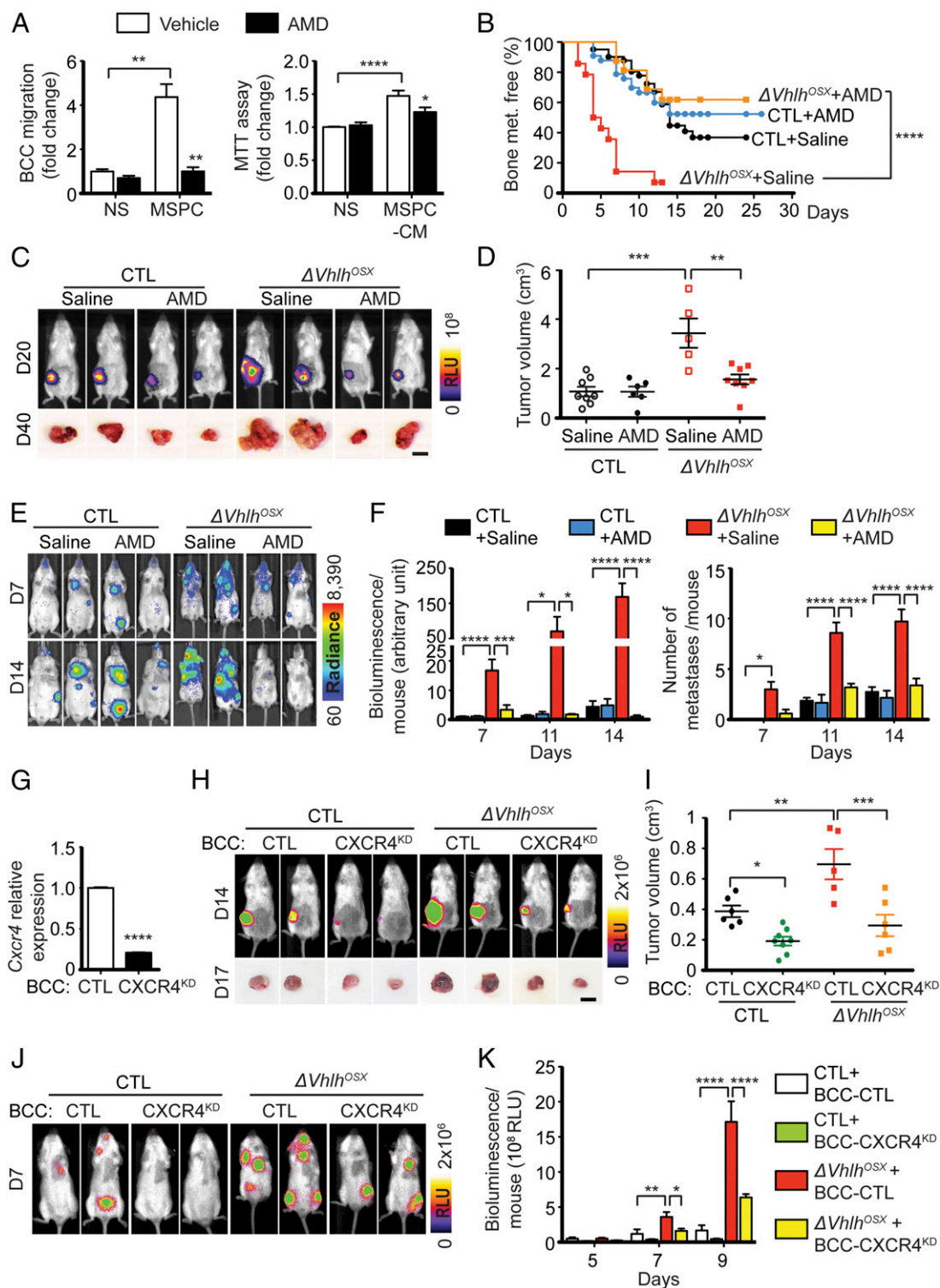


Fig. 6. CXCL12–CXCR4 signaling mediates systemic breast cancer growth and dissemination induced by the skeleton. (A) Migration and MTT assays with BCC-GFP::LUC cells stimulated by MSPCs (Left) or conditioned medium (Right) in presence or absence of the CXCR4 inhibitor AMD3100. Values ($n \geq 4$) are normalized to nonstimulated (NS) controls. (B) Kaplan–Meier analysis of bone metastasis after i.c. injections of BCC-GFP::LUC cells in control mice treated with saline ($n = 31$) or AMD3100 ($n = 37$) and in $\Delta Vhlh^{OSX}$ mice treated with saline ($n = 14$) or AMD3100 ($n = 8$). (C and D) Representative bioluminescent images and tumor photographs obtained after i.f.p. transplantation of BCC-GFP::LUC cells (C) and quantification of tumor volumes at day 40 (control + saline, $n = 8$; control + AMD3100 MD, $n = 6$; $\Delta Vhlh^{OSX}$ + saline, $n = 5$; $\Delta Vhlh^{OSX}$ + AMD3100, $n = 8$) (D). (E and F) Representative images (E) and quantifications of the total bioluminescence and numbers of metastases per mouse (F) after i.c. injections of BCC-GFP::LUC cells ($n \geq 4$ for each group). (G) Relative mRNA expression of *Cxcr4* in BCC-GFP::LUC cells infected with control lentiviruses (BCC-CTL) or with lentiviruses encoding shRNA against *Cxcr4* (BCC-CXCR4^{KD}) ($n = 3$). (H and I) Representative bioluminescence images and tumor photographs (H) and quantifications of tumor volumes (I) 17 d after i.f.p. transplantation of BCC-CTL ($n = 6$ for control; $n = 5$ for $\Delta Vhlh^{OSX}$ mice) or BCC-CXCR4^{KD} ($n = 8$ for control; $n = 6$ for $\Delta Vhlh^{OSX}$ mice). (J and K) Representative images (J) and quantifications of the total bioluminescence per mouse (K) after i.c. injections of BCC-CTL or BCC-CXCR4^{KD} in control or $\Delta Vhlh^{OSX}$ mice ($n \geq 3$ for each group). (Scale bars: 1 cm). Values indicate the mean \pm SEM; * $P < 0.05$, ** $P < 0.01$, *** $P < 0.001$, **** $P < 0.0001$; two-tailed Student's *t* test (A and G), log-rank (Mantel–Cox) test (B), or two-way ANOVA (D, F, I, and K).

Thus, increased bone mass alone is not sufficient to increase tumorigenesis. Conversely, in $\Delta Vhlh^{OSX}$ mice increased bone mass due to increased bone anabolism results in increased tumorigenesis. This supports the concept that increased bone anabolism through increased number and/or biological activity of the osteoblast-lineage cells mediates the tumorigenic effect of the skeleton.

Among all osteoblast-lineage cells, it is still unclear whether immature and differentiated osteoblasts play equal roles in promoting breast cancer growth and metastasis. A recent study indicates that senescent osteoblasts that are terminally differentiated favor bone metastasis (2). However, several arguments support OPCs having a unique role in creating a potent tumorigenic environment. First, we observed that breast cancer cells colonize specific areas particularly enriched in OPCs, while no bone metastases were observed in areas deprived in OPC. Second, genetically targeting OPCs or skeletal mesenchymal progenitor cells in mice is sufficient to induce leukemia or neoplasia of mesenchyme-derived soft tissues locally (37, 38), while these effects are not observed when mature osteoblasts are targeted (17, 38). Third, OPCs, but not mature osteoblasts, express high levels of CXCL12 (8), which increase tumor growth and dissemination (13).

Our work underscores the importance of the HIF signaling activated in osteoblast-lineage cells in breast cancer progression. Interestingly, activation of HIF signaling in mesenchymal progenitor cells upon Prx1-Cre-driven ablation of *Vhlh* results in mesenchymal tumors surrounding synovial joints (37). HIF1 α , but not HIF2 α , triggers this tumorigenic effect in skeletal tissues. Consistent with this observation, we found that deletion of *Hif1 α* , but not *Hif2 α* , in osteoblast-lineage cells severely impaired breast cancer growth and dissemination. The result obtained with $\Delta Hif1\alpha^{OSX}$ mice is important, since it demonstrates that physiological levels of HIF1 activity promote systemic tumorigenesis. Moreover, this suggests that targeting HIF1 signaling in the bone microenvironment could reduce or prevent tumor growth and dissemination in breast cancer.

Cells of the osteoblast lineage secrete several growth factors and cytokines that may influence breast cancer. We identified CXCL12 as a key secreted factor in the systemic control of breast cancer mediated by the skeleton. However, additional factors secreted by osteoblast-lineage cells may play a role. It has been reported that the levels of erythropoietin (EPO) and the number of erythrocytes are increased in $\Delta Vhlh^{OSX}$ mice and that this effect is dependent on HIF2 α but not on HIF1 α (15). Therefore it is conceivable that increased EPO production could increase tumor growth in $\Delta Vhlh^{OSX}$ mice. However, we observed a decreased tumor burden in $\Delta Hif1\alpha^{OSX}$ mice with expected normal EPO levels but not in $\Delta Hif-2\alpha^{OSX}$ mice with expected low EPO levels. This excludes the possibility that physiological levels of bone-derived EPO mediate the systemic breast cancer growth and dissemination induced by the skeleton in our model. Future investigations will likely identify additional bone-derived factors that can generate a systemic tumorigenic environment.

Our results demonstrate that CXCL12 directly stimulates breast cancer cell migration and proliferation, although this does not exclude additional indirect effects. As CXCL12 is a critical regulator of hematopoiesis (39), it may regulate the immune system to influence breast cancer. Interestingly, a recent study indicates that osteoblasts support immune-suppressive myeloid-derived cells, suggesting that osteoblast-lineage cells could indirectly support tumor progression by inhibiting the immune system (40). On the other hand, several publications demonstrate that osteoblasts support the differentiation of several immune cells involved in the antitumoral immune response (41). Further investigation is required to evaluate whether immune responses against tumors are modulated by hypoxic osteoprogenitors.

The clinical relevance of our finding that osteoblast-lineage cells instigate systemic changes promoting tumor growth and dissemination is supported by several clinical studies, which have linked alterations in bone homeostasis with the risk of breast cancer (42–52). High bone mineral density (BMD) has long been associated with increased risk of breast carcinogenesis and increased risk of metastasis in breast cancer patients (42, 44–48, 52). Conversely, low bone mass has been correlated with lower risk of breast cancer and decreased tumor recurrence (43, 49–51). Although BMD was initially thought to reflect a cumulative exposure to estrogens, recent clinical trials demonstrate that high bone mass correlates with elevated breast cancer incidence irrespective of reproductive correlates or endogenous and exogenous exposure to estrogens (44, 46, 47). However, the biological mechanism linking bone mass and the risk of breast cancer is unknown. Although further work is required to evaluate what triggers increased BMD in these patients, our data indicate that increased bone anabolism rather than decreased bone resorption might be responsible. Our data suggest that elevated levels of CXCL12 in bones and plasma could be associated with more advanced breast cancers. Clinical studies report differing results: High CXCL12 plasma levels have been correlated with high-grade tumors of breast cancer patients (53), which supports our observation in mice; on the other hand, low plasma levels in patients have been correlated with increased tumor dissemination (54). Combined measurements of BMD, circulating levels of CXCL12, and clinical signs of cancer progression might help clarify the role of the skeleton and circulating CXCL12 in breast cancer patients.

Collectively, our results indicate that deregulation of bone homeostasis mediated by the osteoblast lineage can significantly affect breast cancer progression and metastasis and underscore the importance of the skeleton as a regulatory organ of the systemic tumor environment. This concept is important clinically, since it suggests that bone anabolic treatments could increase the risk of breast cancer. Future work aimed at identifying molecular targets in the bone may yield novel therapeutic strategies to prevent and treat metastatic disease.

Methods

Mice. All animal protocols were reviewed and approved by the Institutional Animal Care and Use Committee of the University of California, San Francisco and the French National Animal Ethics Committee, CEEA9. Floxed *Vhlh*, floxed *Hif1 α* , floxed *Hif2 α* , and *Osx-Cre::GFP* mice and genotyping protocols have been previously described (23–25, 55). All mice were backcrossed into FVB/n wild-type mice for at least 10 generations. Littermate mice carrying either one copy of the *Osx-Cre::GFP* transgene without the floxed allele or negative for *Osx-Cre::GFP* transgene were used equally as control animals. They were phenotypically indistinguishable and gave identical results in our study.

Breast Cancer Model. Our breast cancer cell (BCC) line was generated from late mammary carcinomas obtained from mouse mammary tumor virus (MMTV)-PyMT transgenic mice (22) that express the PyMT oncoprotein under the control of mouse mammary tumor virus LTR on the pure FVB/n background. This cell line is negative for estrogen receptor (ER) and progesterone receptor (PR) and produces osteolytic bone metastases (Fig. S1). The reporter genes encoding luciferase (pMSCVpuro-Luc) and GFP (pMIG-GFP) were inserted in breast cancer cells to create the BCC-GFP::LUC cell line. Breast cancer cells were inoculated in syngeneic 8-wk-old control and mutant FVB/n mice. Methods for i.c. injection, i.v. (tail vein) injection, and orthotopic i.f.p. transplantation are described elsewhere (56, 57).

Statistics. For all graphics, data are presented as mean \pm SEM. The indicated sample size (*n*) represents the number of mice used for in vivo experiments and the number of independent cell preparations for in vitro experiments. Kaplan–Meier survival curves were compared using the log-rank (Mantel–Cox) test. When comparing the effect of a treatment or different breast cancer cell lines on control and mutant mice, two-way ANOVA was used with Bonferroni posttests. In all other panels, statistical analysis was performed

using an unpaired two-sided Student's *t* test. *P* values are represented as follows: **P* < 0.05; ***P* < 0.01; ****P* < 0.001; *****P* < 0.0001. All statistical analyses were performed using GraphPad Prism software (version 5.0f).

Additional details can be found in *SI Methods*.

ACKNOWLEDGMENTS. We thank all the investigators who generated and made available the floxed/transgenic mice used in these studies: V. Haase (*Vhlh* floxed), R. Johnson (*Hif-1* floxed), and A. McMahon (*Osx-Cre::GFP*); Stanford Photonics for providing the Onyx/M dark box system for in vivo luminescence imaging; J. Ghysdael for providing *shCxcr4* lentiviruses; E. Jaffee for providing NT2.5 cells; A. Ostertag for advice on statistical analyses;

and M. Cohen-Solal for advice on bone histomorphometry. This study was initiated through the support of the University of California, San Francisco Academic Senate Committee on Research Fund 34935/500394 (to S.P.) and was supported by NIH Grants R01 CA057621, R01 CA180039, and U01 CA199315 (to Z.W.), by INSERM, by the Fondation pour la Recherche Contre le Cancer (ARC) as part of the ATIP-AVENIR Program Project Grants R10081H5 and C14007H5 (to S.P.), and by an Association le Cancer du Sein Parlons-en Pink Ribbon Award (to S.P.). C.-S.D. was supported by the French Ministry of Research and the Fondation ARC and was the recipient of the French Society for Mineralized Tissue Biology Award. The funders had no role in the study design, data collection and interpretation, or the decision to submit the work for publication.

- Jones DH, et al. (2006) Regulation of cancer cell migration and bone metastasis by RANKL. *Nature* 440:692–696.
- Luo X, et al. (2016) Stromal-initiated changes in the bone promote metastatic niche development. *Cell Rep* 14:82–92.
- Sterling JA, Edwards JR, Martin TJ, Mundy GR (2011) Advances in the biology of bone metastasis: How the skeleton affects tumor behavior. *Bone* 48:6–15.
- Wang H, et al. (2015) The osteogenic niche promotes early-stage bone colonization of disseminated breast cancer cells. *Cancer Cell* 27:193–210.
- Provot S, Schipani E, Wu J, Kronenberg HM (2008) Development of the skeleton. *Osteoporosis* (Academic, Burlington, MA), 3rd Ed, Vol 1, pp 241–269.
- Maes C, et al. (2010) Osteoblast precursors, but not mature osteoblasts, move into developing and fractured bones along with invading blood vessels. *Dev Cell* 19:329–344.
- Mizoguchi T, et al. (2014) Osterix marks distinct waves of primitive and definitive stromal progenitors during bone marrow development. *Dev Cell* 29:340–349.
- Greenbaum A, et al. (2013) CXCL12 in early mesenchymal progenitors is required for hematopoietic stem-cell maintenance. *Nature* 495:227–230.
- Lee NK, et al. (2007) Endocrine regulation of energy metabolism by the skeleton. *Cell* 130:456–469.
- Oury F, et al. (2011) Endocrine regulation of male fertility by the skeleton. *Cell* 144:796–809.
- Oury F, et al. (2013) Maternal and offspring pools of osteocalcin influence brain development and functions. *Cell* 155:228–241.
- O'Brien CA (2010) Control of RANKL gene expression. *Bone* 46:911–919.
- Guo F, et al. (2016) CXCL12/CXCR4: A symbiotic bridge linking cancer cells and their stromal neighbors in oncogenic communication networks. *Oncogene* 35:816–826.
- Sigl V, Penninger JM (2014) RANKL/RANK—From bone physiology to breast cancer. *Cytokine Growth Factor Rev* 25:205–214.
- Rankin EB, et al. (2012) The HIF signaling pathway in osteoblasts directly modulates erythropoiesis through the production of EPO. *Cell* 149:63–74.
- Shomento SH, et al. (2010) Hypoxia-inducible factors 1 α and 2 α exert both distinct and overlapping functions in long bone development. *J Cell Biochem* 109:196–204.
- Wang Y, et al. (2007) The hypoxia-inducible factor alpha pathway couples angiogenesis to osteogenesis during skeletal development. *J Clin Invest* 117:1616–1626.
- Semenza GL (2012) Hypoxia-inducible factors in physiology and medicine. *Cell* 148:399–408.
- LaGory EL, Giaccia AJ (2016) The ever-expanding role of HIF in tumour and stromal biology. *Nat Cell Biol* 18:356–365.
- Cox TR, et al. (2015) The hypoxic cancer secretome induces pre-metastatic bone lesions through lysyl oxidase. *Nature* 522:106–110.
- Dunn LK, et al. (2009) Hypoxia and TGF-beta drive breast cancer bone metastases through parallel signaling pathways in tumor cells and the bone microenvironment. *PLoS One* 4:e6896.
- Lin EY, et al. (2003) Progression to malignancy in the polyoma middle T oncoprotein mouse breast cancer model provides a reliable model for human diseases. *Am J Pathol* 163:2113–2126.
- Rodda SJ, McMahon AP (2006) Distinct roles for hedgehog and canonical Wnt signaling in specification, differentiation and maintenance of osteoblast progenitors. *Development* 133:3231–3244.
- Ryan HE, Lo J, Johnson RS (1998) HIF-1 alpha is required for solid tumor formation and embryonic vascularization. *EMBO J* 17:3005–3015.
- Haase VH, Glickman JN, Socolovsky M, Jaenisch R (2001) Vascular tumors in livers with targeted inactivation of the von Hippel-Lindau tumor suppressor. *Proc Natl Acad Sci USA* 98:1583–1588.
- Reilly RT, et al. (2000) HER-2/neu is a tumor rejection target in tolerized HER-2/neu transgenic mice. *Cancer Res* 60:3569–3576.
- Xiong J, et al. (2011) Matrix-embedded cells control osteoclast formation. *Nat Med* 17:1235–1241.
- Shinkai I, Ohta Y (1996) New drugs—Reports of new drugs recently approved by the FDA. *Alendronate*. *Bioorg Med Chem* 4:3–4.
- Ceradini DJ, et al. (2004) Progenitor cell trafficking is regulated by hypoxic gradients through HIF-1 induction of SDF-1. *Nat Med* 10:858–864.
- Du R, et al. (2008) HIF1 α induces the recruitment of bone marrow-derived vascular modulatory cells to regulate tumor angiogenesis and invasion. *Cancer Cell* 13:206–220.
- Hitchon C, et al. (2002) Hypoxia-induced production of stromal cell-derived factor 1 (CXCL12) and vascular endothelial growth factor by synovial fibroblasts. *Arthritis Rheum* 46:2587–2597.
- Zou D, et al. (2012) Blood vessel formation in the tissue-engineered bone with the constitutively active form of HIF-1 α mediated BMSCs. *Biomaterials* 33:2097–2108.
- Sánchez-Martín L, Sánchez-Mateos P, Cabañas C (2013) CXCR7 impact on CXCL12 biology and disease. *Trends Mol Med* 19:12–22.
- DiPersio JF, Uy GL, Yasothan U, Kirkpatrick P (2009) Plerixafor. *Nat Rev Drug Discov* 8:105–106.
- Kalatskaya I, et al. (2009) AMD3100 is a CXCR7 ligand with allosteric agonist properties. *Mol Pharmacol* 75:1240–1247.
- Karsenty G, Olson EN (2016) Bone and muscle endocrine functions: Unexpected paradigms of inter-organ communication. *Cell* 164:1248–1256.
- Mangiavini L, et al. (2015) Fibrosis and hypoxia-inducible factor-1 α -dependent tumors of the soft tissue on loss of von Hippel-Lindau in mesenchymal progenitors. *Am J Pathol* 185:3090–3101.
- Raaijmakers MH, et al. (2010) Bone progenitor dysfunction induces myelodysplasia and secondary leukaemia. *Nature* 464:852–857.
- Nagasawa T (2015) CXCL12/SDF-1 and CXCR4. *Front Immunol* 6:301.
- Rosnagl S, et al. (2016) EDA-fibronectin originating from osteoblasts inhibits the immune response against cancer. *PLoS Biol* 14:e1002562.
- Panaroni C, Tzeng YS, Saeed H, Wu JY (2014) Mesenchymal progenitors and the osteoblast lineage in bone marrow hematopoietic niches. *Curr Osteoporosis Rep* 12:22–32.
- Buist DS, LaCroix AZ, Barlow WE, White E, Weiss NS (2001) Bone mineral density and breast cancer risk in postmenopausal women. *J Clin Epidemiol* 54:417–422.
- Cauley JA, et al.; Study of Osteoporotic Fractures Research Group (1996) Bone mineral density and risk of breast cancer in older women: The study of osteoporotic fractures. *JAMA* 276:1404–1408.
- Chen Z, et al.; Women's Health Initiative Program; National Heart, Lung and Blood Institute; US Department of Health and Human Services (2008) Hip bone density predicts breast cancer risk independently of Gail score: Results from the Women's Health Initiative. *Cancer* 113:907–915.
- Fraenkel M, et al. (2013) Association between bone mineral density and incidence of breast cancer. *PLoS One* 8:e70980.
- Hadji P, et al. (2007) Bone mass and the risk of breast cancer: The influence of cumulative exposure to oestrogen and reproductive correlates. Results of the Marburg breast cancer and osteoporosis trial (MABOT). *Maturitas* 56:312–321.
- Kalder M, et al. (2011) Breast cancer and bone mineral density: The Marburg breast cancer and osteoporosis trial (MABOT II). *Climacteric* 14:352–361.
- Kim BK, et al. (2014) Bone mineral density and the risk of breast cancer: A case-control study of Korean women. *Ann Epidemiol* 24:222–227.
- Olsson H, Hägglund G (1992) Reduced cancer morbidity and mortality in a prospective cohort of women with distal forearm fractures. *Am J Epidemiol* 136:422–427.
- Persson I, Adami HO, McLaughlin JK, Naessén T, Fraumeni JF, Jr (1994) Reduced risk of breast and endometrial cancer among women with hip fractures (Sweden). *Cancer Causes Control* 5:523–528.
- Zambetti A, Tartter PI (2013) Bone mineral density is a prognostic factor for postmenopausal caucasian women with breast cancer. *Breast J* 19:168–172.
- Zhang Y, et al. (1997) Bone mass and the risk of breast cancer among postmenopausal women. *N Engl J Med* 336:611–617.
- Potter SM, et al. (2009) Systemic chemokine levels in breast cancer patients and their relationship with circulating menstrual hormones. *Breast Cancer Res Treat* 115:279–287.
- Hassan S, Baccarelli A, Salvucci O, Basik M (2008) Plasma stromal cell-derived factor-1: Host derived marker predictive of distant metastasis in breast cancer. *Clin Cancer Res* 14:446–454.
- Gruber M, et al. (2007) Acute postnatal ablation of Hif-2 α results in anemia. *Proc Natl Acad Sci USA* 104:2301–2306.
- Arguello F, Baggs RB, Frantz CN (1988) A murine model of experimental metastasis to bone and bone marrow. *Cancer Res* 48:6876–6881.
- Kocatürk B, Versteeg HH (2015) Orthotopic injection of breast cancer cells into the mammary fat pad of mice to study tumor growth. *J Vis Exp* 96:e51967.